

Temperature variation across an optical fiber laser: why it is almost always small

Arash Mafi

*Department of Physics & Astronomy and Center for High Technology Materials,
University of New Mexico,
Albuquerque, New Mexico 87131, USA
mafi@unm.edu*

(Dated: February 18, 2020)

It is shown using general arguments that at any location along an optical fiber laser or amplifier, the temperature variation across the fiber is two to three orders of magnitude smaller than the difference between the fiber surface temperature and the ambient temperature. Therefore, the fiber heats almost uniformly in its transverse cross-section regardless of how hot it gets relative to its surroundings, and regardless of how the temperature varies along the fiber. The analysis applies to a broad range of fiber laser and amplifier designs subject to convective air-cooling but can be readily adapted to other forms of cooling.

I. INTRODUCTION

The power generated from optical fiber lasers and amplifiers has increased significantly over the past decade [1–4]. Consequently, efficient heat mitigation has become one of the main concerns, especially in light of recent reports of limitations in power scaling because of the thermally-induced mode instability, which degrades the output beam quality [5–8]. In this brief paper, we argue that the temperature variation across an optical fiber laser is very small, even when the fiber becomes quite hot. Therefore, any consequential thermo-optic effect, e.g., changes in the refractive index due to the temperature variation and the resulting mode-coupling, is almost always a longitudinal phenomenon. The rest of this paper is to establish this argument in broad terms for the double-cladding fiber (DCF) design, which is the primary platform for high-power lasers and amplifiers. The results can be readily applied to the single-cladding design of a core-pumped fiber as a special case.

A schematic transverse profile of the DCF is shown in Fig.1, where we assume a cylindrical geometry for the fiber. The core, in which the signal propagates, is marked with the inner white-filled circle of radius a and is doped with rare-earth ions (typically Yb). The inner cladding, in which the pump propagates, is the region marked with the light-gray region of radius b_i . Of course, some of the propagating pump power overlaps the core region, which is responsible for pumping the core. The outer cladding of the fiber is the region shaded in dark-gray with radius b_o , where $D_o = 2b_o$ is the total outer diameter of the fiber. We also mark the temperature of the center of the fiber core as T_0 , at the core-inner cladding boundary as T_a , at the inner-outer cladding boundary as T_{b_i} , and the outer surface of the fiber as T_{b_o} . The ambient room temperature is identified as T_∞ .

Before, we start our analysis, we would like to present the key result obtained in this paper:

$$\delta T_o = \mathfrak{X} \frac{D_o}{D_{th}} \Delta T. \quad (1)$$

Here, $\delta T_o = T_0 - T_{b_o}$ is the difference between the core

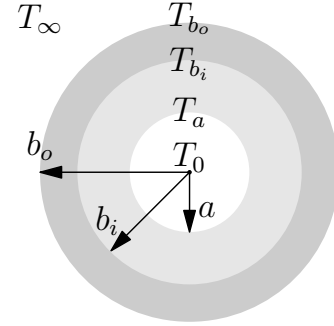


FIG. 1. Schematic of a DCF with temperature markings.

temperature and the surface temperature of the fiber (interior temperature variation), and $\Delta T = T_{b_o} - T_\infty$ is the difference between the surface temperature of the fiber and the ambient temperature. We also have:

$$D_{th} = \frac{4\kappa}{H}, \quad (2)$$

where κ is the thermal conductivity of the (fused silica) glass in units of $W/(m.K)$ and H is the convective heat transfer coefficient in units of $W/(m^2.k)$. \mathfrak{X} is an order one coefficient that is to be determined and depends on the geometrical and optical properties of the laser or amplifier. We will argue that because D_{th} , which is a characteristic length scale obtained from the thermal coefficients, is typically 2-3 orders of magnitude larger than the outer diameter of the fiber (D_o), the temperature variation inside the fiber (δT_o) remains smaller than ΔT by 2-3 orders of magnitude. Conversely, because the fiber surface cannot be feasibly hotter than a few hundred degrees Celsius ($\Delta T \lesssim 500^\circ C$), the temperature variation inside the fiber must be at most a few degrees Celsius, and often lower.

II. FORMULATION

In this paper, we will refer to the pump laser as the “pump”, and to the generated laser (in a laser design) or

the amplified laser (in an amplifier design) as the “signal”. To present our arguments and observations in as general a form as possible without resorting to unnecessary numerical analysis in specific designs, we make several simplifying assumptions. First, we assume that the signal propagates only in the core and is of a top-hat form. In practice, for a conventional DCF, the signal beam profile is nearly Gaussian, and some of its power resides in the inner cladding. This assumption can be made more accurate by including a signal core overlap-factor, which we will not do in the interest of simplicity and generality. Therefore, the signal intensity in the core is I_s and the total signal power is P_s , where $P_s = \pi a^2 I_s$. Both the signal intensity and power are assumed to generally depend on the longitudinal coordinate, z , along the fiber. Second, we assume that the pump propagates only in the inner-cladding and has a uniform intensity of I_p , which can also be a function of z . $P_p = \pi b_i^2 I_p$ is the total pump power. This assumption is usually valid if the pump laser is sufficiently scrambled to maintain its uniformity in the transverse plane. We also define the pump overlap factor with the core as $\Gamma := a^2/b_i^2$. In some DCF designs, the circular symmetry of the inner-cladding is broken to improve the transverse uniformity of the pump intensity. Neither of these technicalities affects our general arguments.

We assume that the fiber temperature is constant in time; therefore, the steady state heat equation can be used to determine the temperature distribution, $T(x, y, z)$:

$$\nabla^2 T + \frac{q}{k} = 0, \quad (3)$$

where the heat source density $q(x, y, z)$ is the thermal energy deposited per second at the location (x, y, z) inside the fiber and is in units of W/m^3 . We assume a uniform thermal conductivity across the fiber because the light doping in the core and inner cladding do not change the value of κ in the host glass, substantially. Equation 3, in general, can only be solved numerically. Here, we make another simplifying assumption that the temperature T varies very slowly with z . We will discuss the validity of this assumption later in the Appendix. Therefore, considering the cylindrical symmetry of the problem and ignoring the $\partial_z^2 T$ term in Eq. 3, we arrive at the following differential equation:

$$\frac{\partial^2 T}{\partial \rho^2} + \frac{1}{\rho} \frac{\partial T}{\partial \rho} + \frac{q}{k} = 0, \quad (4)$$

where ρ is the radial coordinate. Both T and q are in general functions of z ; however, in the following discussion, we drop their explicit z -dependence when writing the equations for simplicity, but their z -dependence is always implicitly assumed. Also, because of our assumptions and the geometry of the fiber in Fig. 1, q is piece-wise constant; therefore, the general solution to the second-

order ordinary differential equation 4 is given by:

$$T(\rho) = \mathcal{C}_1 + \mathcal{C}_2 \log(\rho^2) - \frac{q}{4\kappa} \rho^2, \quad (5)$$

where \mathcal{C}_1 and \mathcal{C}_2 are constants of integration. We consider the uniform heat density in the core ($0 \leq \rho \leq a$) to be q_a and in the inner cladding ($a \leq \rho \leq b_i$) to be q_b . In the core, the temperature must be finite everywhere including at $\rho = 0$; therefore, \mathcal{C}_2 must vanish. Moreover, the temperature and its radial derivative must be continuous at each layer. The result is the following temperature profile, $T_0 - T(\rho)$, inside the fiber:

$$\begin{aligned} T_0 - T(\rho) &= \frac{q_a}{4\kappa} \rho^2, \quad 0 \leq \rho \leq a, \\ &= \frac{q_a - q_b}{4\kappa} a^2 \left[1 + \ln\left(\frac{\rho^2}{a^2}\right) \right] + \frac{q_b}{4\kappa} \rho^2, \quad a \leq \rho \leq b_i, \\ &= \frac{q_a - q_b}{4\kappa} a^2 \left[1 + \ln\left(\frac{\rho^2}{a^2}\right) \right] + \frac{q_b}{4\kappa} b_i^2 \left[1 + \ln\left(\frac{\rho^2}{b_i^2}\right) \right], \quad b_i \leq \rho \leq b_o. \end{aligned} \quad (6)$$

We next introduce the temperature variation parameters across the core $\delta T_a = T_0 - T_a$ and the entire fiber $\delta T_o = T_0 - T_{b_o}$:

$$\begin{aligned} \delta T_a &= \frac{q_a}{4\kappa} a^2, \\ \delta T_o &= \frac{q_a - q_b}{4\kappa} a^2 \left[1 + \ln\left(\frac{b_o^2}{a^2}\right) \right] + \frac{q_b}{4\kappa} b_i^2 \left[1 + \ln\left(\frac{b_o^2}{b_i^2}\right) \right]. \end{aligned} \quad (7a, 7b)$$

The total linear heat density generated in the core is given by $Q_a = q_a \pi a^2$. Similarly, the total linear heat density generated in the inner-cladding is given by $Q_b = q_b \pi (b_i^2 - a^2)$. Therefore, we have:

$$(4\pi\kappa) \delta T_a = Q_a, \quad (8a)$$

$$(4\pi\kappa) \delta T_o = (Q_a + Q_b) \left[1 + \ln\left(\frac{b_o^2}{a^2}\right) \right] + Q_p \ln\left(\frac{a^2}{b_i^2}\right), \quad (8b)$$

where we define $Q_p := q_b \pi b_i^2$.

We assume convective boundary condition for the outer surface of the fiber; therefore, the temperature difference between the fiber surface T_{b_o} and ambient air temperature T_∞ is given by

$$\Delta T = T_{b_o} - T_\infty = \frac{Q_a + Q_b}{2\pi b_o H}. \quad (9)$$

We are now ready to simplify the previous equations and the following two relationship will be useful in the process:

$$Q_b = (1 - \Gamma)Q_p, \quad Q_a = (\gamma + \Gamma)Q_p. \quad (10)$$

Γ was previously defined as the the pump overlap factor with the core and the meaning of the coefficient γ will become clear shortly, but for now, Eq. 10 can be used as the definition of γ . We also define $\eta := \ln(b_o^2/b_i^2)$. After a few lines of algebra, we arrive at:

$$\delta T_a = \frac{D_o}{D_{th}} \left[\frac{\Gamma + \gamma}{1 + \gamma} \right] \Delta T, \quad (11a)$$

$$\delta T_o = \frac{D_o}{D_{th}} \left[(1 + \eta) + \frac{\gamma}{1 + \gamma} (-\ln \Gamma) \right] \Delta T, \quad (11b)$$

Equations 11a and especially 11b are the main results of this paper. Note that comparing Eq. 11b to Eq. 1 identifies the parameter \mathfrak{X} as

$$\mathfrak{X} = (1 + \eta) + \frac{\gamma}{1 + \gamma}(-\ln \Gamma). \quad (12)$$

For fused silica at room temperature, we have $\kappa = 1.38 \text{ W}/(\text{m}\cdot\text{K})$. If we assume $H \approx 36.8 \text{ W}/(\text{m}^2\cdot\text{k})$, which is a reasonable value for an air fan-cooled fiber, we obtain $D_{th} = 4\kappa/H \approx 15 \text{ cm}$. Therefore, D_{th} is 2-3 orders of magnitude larger than the outer diameter, D_o , of a conventional fiber laser in Eqs. 11a and 11b. In the next section, we will cover several conventional designs to show that \mathfrak{X} is of order one; therefore, considering that $D_o \ll D_{th}$, we generally have $\delta T_o \ll \Delta T$. We will also discuss the dimensionless coefficient in square brackets in Eq. 11a in these cases, but it is less consequential because we always have $\delta T_a < \delta T_o$.

III. EXAMPLES

In the following, we will examine three examples of Yb-doped optical fibers from Thorlabs Incorporated, where the relevant fiber parameters are given in Table I. We will show that in all three cases \mathfrak{X} is an order one parameter ($\mathfrak{X} < 10$), regardless of the details of the laser or amplifier configuration, and $\delta T_o \ll \Delta T$.

TABLE I. The relevant fiber parameters for Eqs. 11a and 11b.

name	fiber ID	$2a(\mu\text{m})$	$2b_i(\mu\text{m})$	$2b_o(\mu\text{m})$
<i>Fiber1</i>	YB1200-4/125	4		125
<i>Fiber2</i>	YB1200-10/125DC	10	125	245
<i>Fiber3</i>	YB1200-20/400DC	20	400	520

A. Core-pumped fiber laser

The first example that we cover is a core-pumped fiber laser. Both the signal and the pump propagate in the core and there is only a single cladding surrounding the core. This configuration can be obtained as a special example of the DCF in Fig.1 with $b_i = a$, which gives $\Gamma = 1$ and $\eta = \ln(b_o^2/a^2)$. In this case, Eqs. 11a and 11b are simplified to

$$\delta T_a = \frac{D_o}{D_{th}} \Delta T, \quad (13a)$$

$$\delta T_o = \frac{D_o}{D_{th}} (1 + \eta) \Delta T, \quad (13b)$$

A typical example is *Fiber1* from Table I. Using the relevant parameters in the Table, it can be shown that $\eta \approx 6.9$ and $D_{th}/D_o \approx 1200$. We therefore conclude that

$\mathfrak{X} = 1 + \eta \approx 7.9$ and $\delta T_o < 0.0066\Delta T$ and $\delta T_o \approx 7.9\delta T_a$. In other words, no matter how hot the fiber becomes when operating as a laser or amplifier, the temperature variation in the fiber is not more than a couple of degrees Celsius.

B. Cladding-pumped fiber laser

In a conventional cladding-pumped fiber laser, the primary sources of heating are from the quantum defect in the core of the fiber and the parasitic absorption of both the signal and the pump. Based on our assumptions, the heating due to the quantum defect happens uniformly in the core with the linear heat density of Q_{qd} , which only contributes to Q_a . The linear heat density due to the parasitic absorption of the signal is given by $Q_{as} = \alpha_s P_s$, which only contributes to Q_a , as well. The linear heat density due to the parasitic absorption of the pump is given by $Q_{ap} = \alpha_p P_p$, a fraction of which, ΓQ_{ap} , contributes to Q_a and the rest, $(1 - \Gamma)Q_{ap}$, is deposited in the inner cladding and contributes to Q_b . Here, α_s and α_p are the parasitic absorption coefficients of the signal and the pump, respectively. Using these definitions, we obtain:

$$Q_a = Q_{qd} + Q_{as} + \Gamma Q_{ap}, \quad Q_b = (1 - \Gamma)Q_{ap}. \quad (14)$$

Using Eq. 10 and the definitions presented in Eq. 14, it can be easily shown that

$$\gamma = \frac{Q_{qd} + Q_{as}}{Q_{ap}}. \quad (15)$$

Equation 15 makes the meaning of the parameter γ more clear: γ is the ratio of the sum of the quantum defect linear heat density and the signal parasitic absorption, both of which are deposited in the core, to the total parasitic heat generation in the fiber due to the pump. The good news is that we may not need to know much about the relative contributions of Q_{qd} , Q_{as} and Q_{ap} because γ appears in Eq. 11b in the form of $\gamma/(1 + \gamma)$, which is always between 0 and 1, i.e., $0 \leq \gamma/(1 + \gamma) \leq 1$, which sets its contribution to \mathfrak{X} .

For the cladding-pumped fiber laser, we consider two different fibers that are commonly used in high-power fiber lasers and amplifiers: the relevant parameters of *Fiber2* and *Fiber3* are shown in Table I.

For *Fiber2*, we have $\eta \approx 1.35$, $\Gamma \approx 0.0064$, and $-\ln \Gamma \approx 5.05$. We obtain $D_o/D_{th} \approx 1.6 \times 10^{-3}$ and $2.3 \lesssim \mathfrak{X} \lesssim 7.4$, where the variation in \mathfrak{X} comes from the fact that for $0 \leq \gamma < \infty$ in Eq. 15, we have $0 \leq \gamma/(1 + \gamma) \leq 1$ in Eq. 12. Therefore, the value of \mathfrak{X} is largely insensitive to the relative contributions of Q_{qd} , Q_{as} , and Q_{ap} , which makes our conclusions quite general. Using the value of D_o/D_{th} and the range of \mathfrak{X} , we obtain $0.004 \lesssim \delta T_o/\Delta T \lesssim 0.012$. While the ratio of $\delta T_o/\Delta T$, which is the maximum value for the temperature variation in the fiber, is largely insensitive to the value of γ , this is not the case for δT_a ,

which is always smaller than δT_o . In fact, δT_a can be much smaller or comparable to δT_o depending on the relative contributions of Q_{qd} , Q_{as} , and Q_{ap} . For *Fiber2*, we have $0.0027 \lesssim \delta T_a/\delta T_o \lesssim 0.14$, depending on the value of γ .

For *Fiber3*, we obtain $\eta \approx 0.52$, $\Gamma \approx 0.0025$, and $-\ln\Gamma \approx 6$. For this fiber, we obtain $1.5 \lesssim \mathfrak{X} \lesssim 7.5$ and $D_o/D_{th} \approx 3.5 \times 10^{-3}$; therefore, $0.005 \lesssim \delta T_o/\Delta T \lesssim 0.026$. Note that the upper limit is obtained for $\gamma \gg 1$, which is generally the case when the heating from the quantum defect totally overwhelms the contribution from the parasitic absorption of the pump and signal—this limit can be avoided in modern high-power fiber amplifiers by lowering the quantum defect [9] or in nearly radiation-balanced lasers [10–13]. We have $0.0016 \lesssim \delta T_a/\delta T_o \lesssim 0.13$, depending on the value of γ .

In summary, even if the fiber surface is 300°C hotter than the ambient temperature, at most for *Fiber1* we have $\delta T_o < 2^\circ\text{C}$, for *Fiber2* we have $\delta T_o < 3.6^\circ\text{C}$, and for *Fiber3* we have $\delta T_o < 4.8^\circ\text{C}$, and most likely even lower in an actual design, where γ is a finite value. Formally, the range of variation for $\delta T_o/\delta T$ can be obtained from Eq. 11b as

$$(1 + \eta) \frac{D_o}{D_{th}} < \frac{\delta T_o}{\Delta T} < (1 + \eta - \ln\Gamma) \frac{D_o}{D_{th}}, \quad (16)$$

which can be expressed in even a simpler and more intuitive form:

$$\left[1 + \ln(b_o^2/b_i^2)\right] \frac{D_o}{D_{th}} < \frac{\delta T_o}{\Delta T} < \left[1 + \ln(b_o^2/a^2)\right] \frac{D_o}{D_{th}}. \quad (17)$$

Therefore, the range of $\delta T_o/\Delta T$ is determined only by the geometrical and thermal properties of the fiber.

IV. SUMMARY AND CONCLUSION

We have shown that the temperature variation inside an optical fiber laser or amplifier (δT_o) is commonly less than ten degrees Celsius and often even much lower. It is argued, in the most general terms, that δT_o is 2-3 orders of magnitude smaller than the temperature difference between the surface of the fiber and the ambient room temperature (ΔT). Because ΔT cannot be larger than a few hundred degrees Celsius, δT_o must be quite small. The arguments are general and apply to a broad range of fiber lasers and amplifiers. However, there are key assumptions made in the derivations that if violated, warrant a careful reexamination. The first key assumption is the steady-state analysis, so if there are temporally varying and transient phenomena, e.g. in pulsed lasers, the conclusions may not hold. The second assumption is that the thermal conductivity of the fiber is uniform (fused silica glass); however, if the outer cladding is made from a less thermally conductive material, then the smaller value of κ sets the scale in Eq. 2 and would reduce the ratio of $\Delta T/\delta T_o$, proportionally. In such a scenario, especially

if polymers are used for the second cladding, the maximum allowable ΔT may be even lower and the general claim of the paper may hold. The third key assumption is that the fiber is air-cooled using the convection mechanism, such as an air-fan cooled system. If liquid cooling or other methods are used to increase the value of the convective heat transfer coefficient H in Eq. 2 beyond $\sim 100 \text{ W}/(\text{m}^2\cdot\text{k})$, the ratio of $\Delta T/\delta T_o$ would be reduced proportionally. However, the formalism developed here still allows broad conclusions on the temperature distributions regardless of the system design.

APPENDIX A

In this Appendix, we would like to justify the absence of the $\partial_z^2 T$ term in our analysis based on Eq. 4. Let's consider a situation where q in Eq. 3 can be expressed as $q(\rho, z) = \tilde{q}(\rho) f(z)$. This separable form, while very convenient in our analysis, can be fully justified if only one of the heating sources, Q_{qd} , Q_{as} , or Q_{ap} , is the dominant one. However, our discussion captures the essence of why the $\partial_z^2 T$ term can be ignored, regardless.

The analysis presented in this paper means that the temperature profile has a ρ -dependence subject to the form of Eq. 4 with $\tilde{q}(\rho)$ as the heat source, and a z -dependence of the form $f(z)$. In other words, $T(\rho, z) \approx \tilde{T}(\rho) f(z)$, where

$$\frac{\partial^2 \tilde{T}(\rho)}{\partial \rho^2} + \frac{1}{\rho} \frac{\partial \tilde{T}(\rho)}{\partial \rho} + \frac{\tilde{q}(\rho)}{k} = 0. \quad (18)$$

Without making any approximations, the full form of the temperature profile can be expressed as

$$T(\rho, z) = \tilde{T}(\rho) f(z) + \tau(\rho, z), \quad (19)$$

where $\tau(\rho, z)$ should be negligible if our approximations hold. In other words, the size of $\tau(\rho, z)$ characterizes the relative importance of keeping the $\partial_z^2 T$ term in Eq. 3.

If we substitute $T(\rho, z)$ from Eq. 19 in Eq. 3, while considering Eq. 18, we arrive at

$$\nabla^2 \tau(\rho, z) + \tilde{T}(\rho) \partial_z^2 f(z) = 0. \quad (20)$$

In Eq. 20, the term $\partial_z^2 f(z)$ can be approximated into the form of $f(z)/\tilde{L}$, where \tilde{L} is a length-scale on the order of the full length of the optical fiber. This can be understood for example if $f(z) \sim \exp(-\tilde{\alpha} z)$, where $\tilde{\alpha}$ can be, e.g., the absorption coefficient of the pump, and the pump power is almost entirely absorbed over the full length of the fiber laser. If the pump power is not fully absorbed, then \tilde{L} can be even larger than the length of the optical fiber. Next, looking at Eq. 6 reveals that the radial temperature profile of the fiber has, generally speaking, the form of $\tilde{T}(\rho) \sim \tilde{\rho}^2 \tilde{q}(\rho)/4\kappa$, where $\tilde{\rho}^2$ is a length scale comparable to the radius of the fiber. Therefore, we can approximate Eq. 20 as

$$\nabla^2 \tau(\rho, z) + \frac{\tilde{\rho}^2}{\tilde{L}^2} \frac{\tilde{q}(\rho) f(z)}{k} = 0. \quad (21)$$

Comparing Eq. 21 with Eq. 18, it can be readily observed that

$$\tau(\rho, z) \sim \frac{\tilde{\rho}^2}{\tilde{L}^2} \tilde{T}(\rho) f(z), \quad (22)$$

therefore, $\tau(\rho, z)$ is smaller than $\tilde{T}(\rho) f(z)$ by the factor of $\tilde{\rho}^2/\tilde{L}^2$, which is usually 4 orders of magnitude or more.

In summary, $\partial_z^2 T$ term can be ignored unless longitudinal variations in heat deposit in the fiber occur at scales comparable to the fiber diameter, which is hardly

conceivable.

FUNDING INFORMATION

This material is based upon work supported by the Air Force Office of Scientific Research under award number FA9550-16-1-0362 titled Multidisciplinary Approaches to Radiation Balanced Lasers (MARBLE).

-
- [1] L. Zenteno, “High-power double-clad fiber lasers,” *J. Light. Technol.* **11**, 1435–1446 (1993).
 - [2] D. J. Richardson, J. Nilsson, and W. A. Clarkson, “High power fiber lasers: current status and future perspectives [invited],” *J. Opt. Soc. Am. B* **27**, B63–B92 (2010).
 - [3] M. N. Zervas and C. A. Codemard, “High power fiber lasers: a review,” *IEEE J. Sel. Top. Quantum Electron.* **20**, 219–241 (2014).
 - [4] F. Beier, C. Hupel, S. Kuhn, S. Hein, J. Nold, F. Proske, B. Sattler, A. Liem, C. Jauregui, J. Limpert, N. Haarlammert, T. Schreiber, R. Eberhardt, and A. Tünnermann, “Single mode 4.3 kW output power from a diode-pumped Yb-doped fiber amplifier,” *Opt. Express* **25**, 14892–14899 (2017).
 - [5] Arlee V. Smith and Jesse J. Smith, “Mode instability in high power fiber amplifiers,” *Opt. Express* **19**, 10180–10192 (2011).
 - [6] B. Ward, C. Robin, and I. Dajani, “Origin of thermal modal instabilities in large mode area fiber amplifiers,” *Opt. Express* **20**, 11407–11422 (2012).
 - [7] C. Jauregui, T. Eidam, H.-J. Otto, F. Stutzki, F. Jansen, J. Limpert, and A. Tünnermann, “Physical origin of mode instabilities in high-power fiber laser systems,” *Opt. Express* **20**, 12912–12925 (2012).
 - [8] V. Scarnera, F. Ghiringhelli, A. Malinowski, C. A. Codemard, M. K. Durkin, and M. N. Zervas, “Modal instabilities in high power fiber laser oscillators,” *Opt. Express* **27**, 4386–4403 (2019).
 - [9] R. Li, H. Xiao, J. Leng, Z. Chen, J. Xu, J. Wu, and P. Zhou, “2240 W high-brightness 1018 nm fiber laser for tandem pump application,” *Laser Physics Letters* **14**, 125102 (2017).
 - [10] S. R. Bowman, S. P. O’Connor, S. Biswal, N. J. Condon, and A. Rosenberg, “Minimizing heat generation in solid-state lasers,” *IEEE J. Quantum Electron.* **46**, 1076–1085 (2010).
 - [11] S. R. Bowman, “Low quantum defect laser performance,” *Optical Engineering* **56**, 011104 (2016).
 - [12] E. Mobini, M. Peysokhan, B. Abaie, and A. Mafi, “Thermal modeling, heat mitigation, and radiative cooling for double-clad fiber amplifiers,” *J. Opt. Soc. Am. B* **35**, 2484–2493 (2018).
 - [13] E. Mobini, M. Peysokhan, and A. Mafi, “Heat mitigation of a core/cladding Yb-doped fiber amplifier using anti-Stokes fluorescence cooling,” *J. Opt. Soc. Am. B* **36**, 2167–2177 (2019).